Chapter 2: Molecular Magnetic Materials

Interplay of chiral auxiallary ligand and azide bridging ligand during the coordiantion network formation with Copper (II)

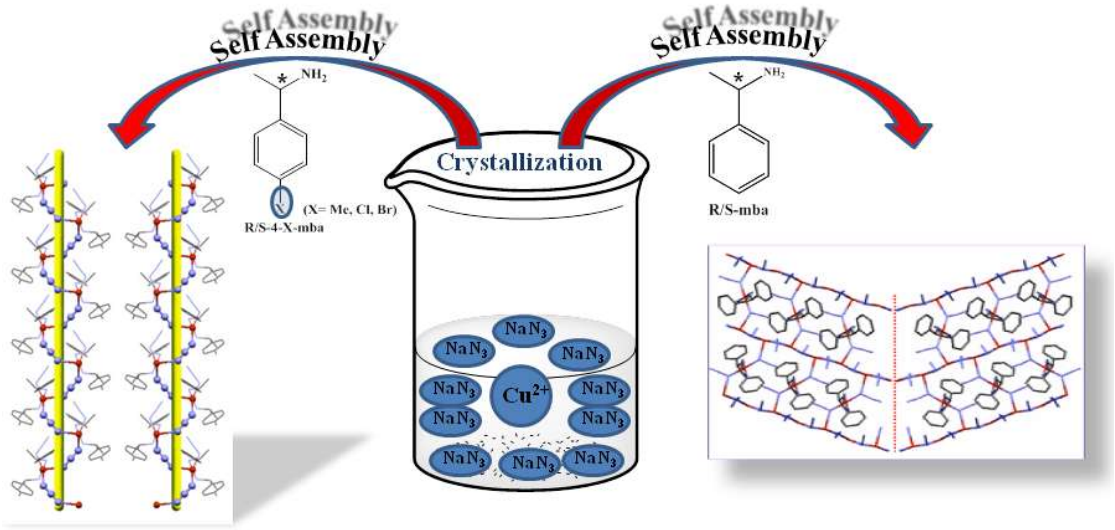

The magnetic behavior of a material depends on presence of 'unpaired electron' dictated by its structure largely in accordance with electronic configuration, and temperature. Interestingly, 'single' or 'unpaired' electrons mostly resided in 'd'/'f' orbitals of atom, show tendency to get or remain oriented in a direction with respect to external magnetic field, resulting in 'ferro' or antiferromagnetism, a bulk property useful in present and future 'technology'[1]. In this aspect, a molecule (or molecular ion) instead of atom (or caion/metal/metal oxides) presents an exciting prospect due to (i) easy modulation of the magnetic properties by energy efficient low temperature organic synthetic methodologies leading to plethora of possible structures, and (ii) convenient combination of magnetic properties with other physical properties (electrical and optical) [2]. Therefore, Molecular magnetism, delocalized electronic system, demand designing and syntheses of diverse molecular systems with detailed focus on structure-property relationship [3].

The first molecular compounds with spontaneous magnetization below a critical temperature were reported during 1990's [4]. A lot of renewed technological interest in this field of research has increased from magneto-optical devices to spintronics. A class of compounds coming under these techno-initiatives are single molecule magnets, and organic-inroganic hybrid compounds for multifunctional or multiferroic behaviour. Magnetism is a bulk property; therefore there should be exchange between building blocks, or 'spin' compartments, so as to achieve long range ordering. Oxamato, oxamido, oxalate, cyanide, and azide-bridges in compounds or systems play an important role of molecular communicator to make 'magnetism' achieved at molecular level. The most extensively used spin carriers are metal (*d*-orbital) and/or radicals (*p*-orbitals). Controlling the dimensional aspect to achieve bulk property with a proper metal center-molecular mediator 'combination' is still a challenge, and therefore, need of crystal engineering or design is amongst the most viable option.

Our Interest: Effective use of molecular chirality for building structure and hence magnetic property.

Interplay of chiral auxiallary ligand and azide bridging ligand during the cocordiantion network formation with Copper (II)

Abstract:

Self assembly formation of bridging ligand and chiral auxiliary ligand with metal centre, in general, gets dominated by metal-bridging ligand interaction. We report here that by introduction of weak non-covalent interactions away from chiral centre can manifest molecular chirality in an auxiliary ligand into the self assembled structure. Details of azido bridged copper (II) coordination networked structures with chiral and achiral benzylamine derivatives are discussed. Five new inorganic-organic coordination compounds,; [Cu ((*R*)-4-Me mba)$_2$ $(N_3)_2]_n$ (**1**) , [Cu ((*S*)-4-Me mba)$_2$ $(N_3)_2]_n$ (**2**) , [Cu ((*R*)-4-Cl mba)$_2$ $(N_3)_2]_n$ (**3**) , [Cu ((*S*)-4-Cl mba)$_2$ $(N_3)_2]_n$ (**4**) and [Cu ((*R*)-4-Br mba)$_2$ $(N_3)_2]_n$ (**5**) (mba- methyl benzylamine), in which Cu (II) azido inorganic motifs are interlinked into 1-dimensional networks have been synthesized, by use of a series of para substituted methyl benzylamine-type building blocks. Interestingly, methyl benzylamine and ethyl benzyl amines are known to form 2-D brick walled motif. The crystal structure of all compounds shows Cu (II) ion in distorted square based pyramid shape, in which axial position is occupied by one nitrogen atom of the azide bridge (EE mode) and the equatorial plane is formed by nitrogen atoms from the two amine ligands and the nitrogen atom of the EO azide. We observed presence of CH-π and X---N interactions are useful in dictating the geometry and dimensionality of the copper (II) azido network. Compounds 1-5 are 1-D confirms the correlation between the helicity of 1-D chains and the chirality of building blocks using CD spectra measurements.

2.1 Introduction

Chirality is one of the most promising and unique properties of a molecule and plays a vital role in living systems and for the rational design of functional materials in modern technology [5]. Chiral organic molecules are used as auxiliary ligands in the synthesis of multifunctional molecular magnets to obtain noncentrosymmetric structures [6]. However, in most cases, the structural chirality does not significantly influence the bulk properties such as magnetism, chiral recognition [7]. One of the reasons could be that the chirality in the ligand does not directly act as a "superexchange" or "bridging" between two metal centers. This is because the most common bridging ligands are small, such as cyanide, azide, or hydroxyl, making it challenging to incorporate chirality in them [8]. Therefore, a commonly adopted strategy is to use achiral auxiliary ligand (CAL) with a chiral center near the metal center. But this strategy actually hinders "free interaction" or the self-assembly process between two adjacent chiral centers present on auxiliary ligand, making it difficult to transfer molecular chirality into the coordination network [6,7].

A one-pot method is commonly adapted for the synthesis of coordination networks where the self-assembly process dictates the metal ions geometry and hence overall dimensionality [9]. During the formation of self-assembly and crystallization of coordination networked structures, three types of interactions compete, namely, (a) metal-bridging ligand interaction, (b) metal-auxiliary ligand complexation, and (c) the inter-ionic and noncovalent interaction among auxiliary ligands. However, the literature is mostly focused on designs based on the first two interactions toward controlling the structures. One will naively expect a significant contribution of the third interaction when the ligand is chiral, chiral auxiliary ligand (CAL). But the impact of the chirality of ligands in the formation of coordination networks has not received the required attention [10].

Although metal compounds with CALs are extensively reported in the literature, the CAL−CAL interactions are not consciously investigated. To the best of our knowledge, this is the first report where an inherent chirality in a ligand is "effectively" used to modify the overall self-assembly process and coordination network structure. This strategy will help in designing compounds with magnetochiral dichroism (MChD)

effects, yet a challenge in molecular materials and chiral recognition of substrates.

The present investigation highlights the self-assembly driven coordination complex formation reaction between Cu^{2+} as a metal center with azide as a bridging ligand and derivatives of α-methylbenzylamine as CAL [11]. It was observed that when achiral benzylamine was used as an auxiliary ligand (AL), it gets attached to Cu(II) with a distorted square planar structure which in turn is a part of a two-dimensional (2-D) sheet formed by two μ-1,1- (end-on, *EO*) and two μ-1,3- (end-to-end, *EE*) coordinated azide molecules between a distorted square pyramidal Cu^{2+} center [12]. An *EO* azide bridge is observed between two Cu^{2+} cations leading to ferromagnetic behavior of this compound. Even after the introduction of chirality at the pro-chiral center, insertion of a methyl group or ethyl group at a benzylic position, the overall structure of the compound remains similar to that of the achiral compound [13]. This indicates the chiral center present near the metal center "does not influence" the self-assembly process, and the final structure is driven by metal-bridging ligand interactions only. The major difference in the achiral and chiral compound is that the latter compounds exhibit characteristic circular dichroism (CD) spectra, although chirality is not observed in the structure.

To make a CAL effective, we inserted a hydrogen bond acceptor group at the para-position on the chiral methyl benzylamine ligand. As per our expectation, chirality is observed in the crystal structure in the form of a one dimensional (1-D) helical chain, with the presence of only *EE* azide bridged networked structures, as discussed below. To observe the interplay between two ligands, we supported the present work by using an enantiomerically pure and admixture of CAL's.

Thus, to understand the roles played by CAL and bridging ligands, three separate sets of experiments were planned. In all these experiments the ratio of metal: bridging ligand to CAL was kept 1:10:0.5 in mole equivalents. Experiment-I was devised to understand the effect of substitution away from the chiral center in enantiomerically pure CAL. Here, we used three derivatives, total five, of methyl benzyl amines as CAL 4-methyl-α-methylbenzylamine (4-Memba: two enantiomers *R* and *S* as **1** and **2**), 4-chloro-α-methylbenzylamine (4-Clmba: two enantiomers *R* and *S* as **3** and **4** respectively), 4-bromo-α-methylbenzylamine (4-Brmba: one enantiomers *R* as **5**), to obtain complexes in the form of single crystals as **1**[Cu((*R*)-4-Memba)$_2$(N$_3$)$_2$]$_n$ and **2**[Cu((*S*)-4-

Memba)$_2$(N$_3$)$_2$]$_n$, **3** [Cu((*R*)-4-Clmba)$_2$(N$_3$)$_2$]$_n$ and **4** [Cu((*S*)-4-Clmba)$_2$(N$_3$)$_2$]$_n$ and **5** [Cu((*R*)-4-Brmba)$_2$(N$_3$)$_2$]$_n$ respectively. Experiment II was devised to understand the self-assembly behavior in a racemic mixture of CAL over their enantiopure form which is discussed in chapter 5-part II in which we carried out two experiments separately on racemic mixtures of 4-chloro-α-methylbenzylamine (**L3**$_{\boldsymbol{RS}}$) and α-methylbenzylamine (**L**$_{\boldsymbol{RS}}$). Experiment III was undertaken to understand competition between two CALs during the process of crystallization. Here we used an equivalent mixture of enantiomerically pure (*R*)-4-chloro-α-methylbenzylamine (**L3**) and (*R*)-α-methylbenzylamine (**L**) as CAL.

2.2 Experimental

2.2.1 Materials and Methods:

All reagents were commercially purchased. (*R*)-(+)-4-methyl-*α*-methyl benzylamine, (*S*)-(-)-4-methyl-*α*-methyl benzylamine, (*R*)-(+)-4-chloro-*α*-methyl benzylamine, (*S*)-(-)-4-chloro-*α*-methyl benzylamine and (*R*)-(+)-4-bromo-*α*-methylbenzylamine were from Aldrich and other analytical-grade chemicals were from Qualigens (Fischer Scientific) and used without further purification. The copper nitrate trihydrate was obtained from Merck; doubly deionized water was used for the synthesis.

2.2.2 Syntheses of compounds:

Scheme: 1.1

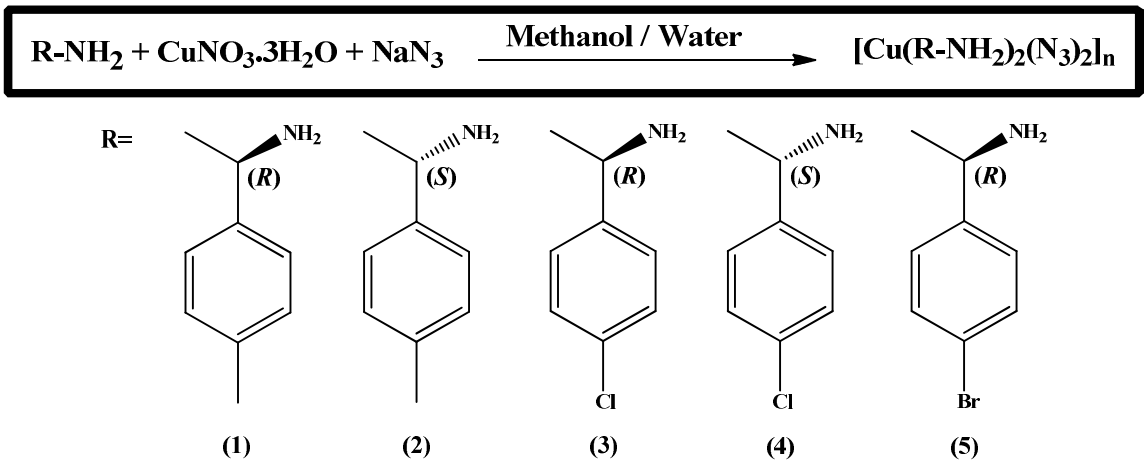

A methanolic solution (10 mL) containing copper (II) nitrate trihydrate (0.2 mmol) was mixed with an aqueous solution of sodium azide (130 mg, 2 mmol) dissolved in a minimum volume of water. (*R*)- (+)-4-methyl methyl benzylamine and (0.1 mmol) in 3 mL of methanol was added to this reaction mixture with continuous stirring. The resulting dark-green solution was filtered and left to stand at room temperature. Dark green plate-shaped crystals of **1** suitable for X-ray diffraction were obtained by slow evaporation of the solvents within 1 week.

Compound **2, 3, 4** and **5** were obtained using a similar method to that of **1**, by employing (*S*)-(-)-4-methyl methyl benzylamine, (*R*) - (+) 4-chloro-*α*-methyl benzylamine, (*S*)-(-)-4-chloro methyl benzylamine, (*R*)-(+)-4-bromo methyl benzylamine, respectively. Yield of single crystals was around 50%.

2.3 Result and Discussions

2.3.1 FT-IR:

FT-IR spectra of all azide compounds were recorded at RT. It showed as expected similar features for **1**/**2**, **3**/**4** and **5** as shown in Figure 2.1.

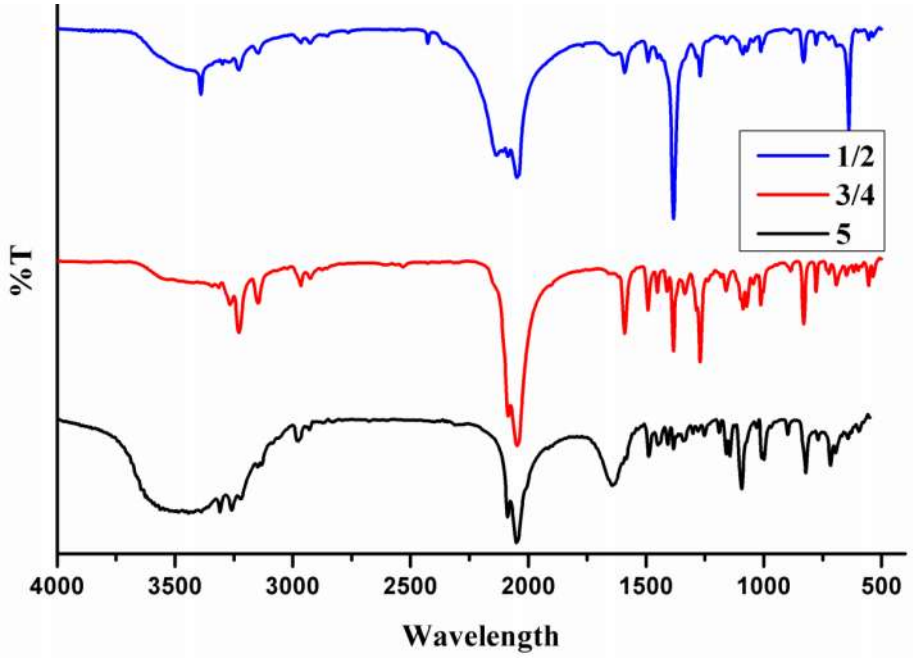

Fig. 2.1: FT-IR of compound 1/2, 3/4 and 5

Compound 1 and 2- FT-IR (KBr): 3232(w), 3067(w),2980 (m), 2935(m), 2081(s), 2050(s), 1610(s), 1560(s), 1500(s), 1429 (s), 1347(s), 1215(s), 1071(s), 1021(s), 928(m), 810 (s).

Compound 3 and 4- FT-IR (KBr): 3314(m), 3265(s), 3228(m), 2965(m), 2085(s), 2047(s), 1591(s), 1492(s), 1452 (m), 1384(s), 1270(s), 1160(m), 1089(m), 1012(m), 830(s), 778 (m), 692(m).

Compound 5- FT-IR (KBr): 3308(m), 3258(m), 3222(s), 2975(s), 2933 (w), 2831(w), 2084(s), 2048(s), 1639(s), 1487(s), 1445(s), 1379(m), 1250(w), 1189(m), 1095(s), 1034(s), 896(m), 823(s), 767 (m), 642(m).

It is observed that $-NH_2$ symmetric and antisymmetric stretching observed in the range of 3213-3314 cm^{-1} in all complexes. Aliphatic $-CH_3$ stretching band observed around in the range of 2980-2965 cm^{-1} while $-CH_3$ symmetric deformation mode observed at the range

of 1384-1347 cm^{-1} and at 1270-1250 cm^{-1}. Modes at 2081-2085 cm^{-1} and 2047-2050 cm^{-1} confirmed the azide binding frequency. C-H ring stretching modes were observed at the range of 1429-1639 cm^{-1}. Bands at the range of 1347-1384 cm^{-1} indicate the C-N stretching mode. *in- plane* CH deformation modes were observed at the range of 1012-1215 cm^{-1} while out-of-plane deformation modes at the range of 642-778 cm^{-1}. Bands at the range of 896-928 cm^{-1} was attributed to -CH_2 *rocking* mode. Sharp medium bands were observed at 767-778 cm^{-1} assigned to the *out-of- plane* ring deformation.

2.3.2 Elemental analyses:

The calculated elemental analyses were consistent with the observed formulae of azide compounds.

Compound 1: Anal. Calc. for $C_{18}H_{26}CuN_8$: C, 51.67; H, 6.21; N, 26.79%; **Found:** C, 50.89; H, 6.14; N, 27.01%.

Compound 2: Anal. Calc. for $C_{18}H_{26}CuN_8$: C, 51.67; H, 6.21; N, 26.79%; **Found:** C, 51.13; H, 6.10; N, 26.80%.

Compound 3: Anal. Calc. for $C_{16}H_{20}Cl_2CuN_8$: C, 41.84; H, 4.35; N, 24.40%. **Found:** C, 41.36; H, 4.30; N, 24.61%.

Compound 4: Anal. Calc. for $C_{16}H_{20}Cl_2CuN_8$: C, 41.84; H, 4.35; N, 24.40%; **Found:** C, 41.23; H, 4.29; N, 24.57%.

Compound 5:**Anal. Calc. for** $C_{16}H_{20}Br_2CuN_8$: C, 35.05; H, 3.65; N, 20.44%; **Found: C,** 35.43; H, 3.62; N, 20.57%.

2.4 Thermal Studies

Thermo-gravimetric studies were carried out for the compounds **1-5** in nitrogen atmosphere in the 303-823 K temperature range.

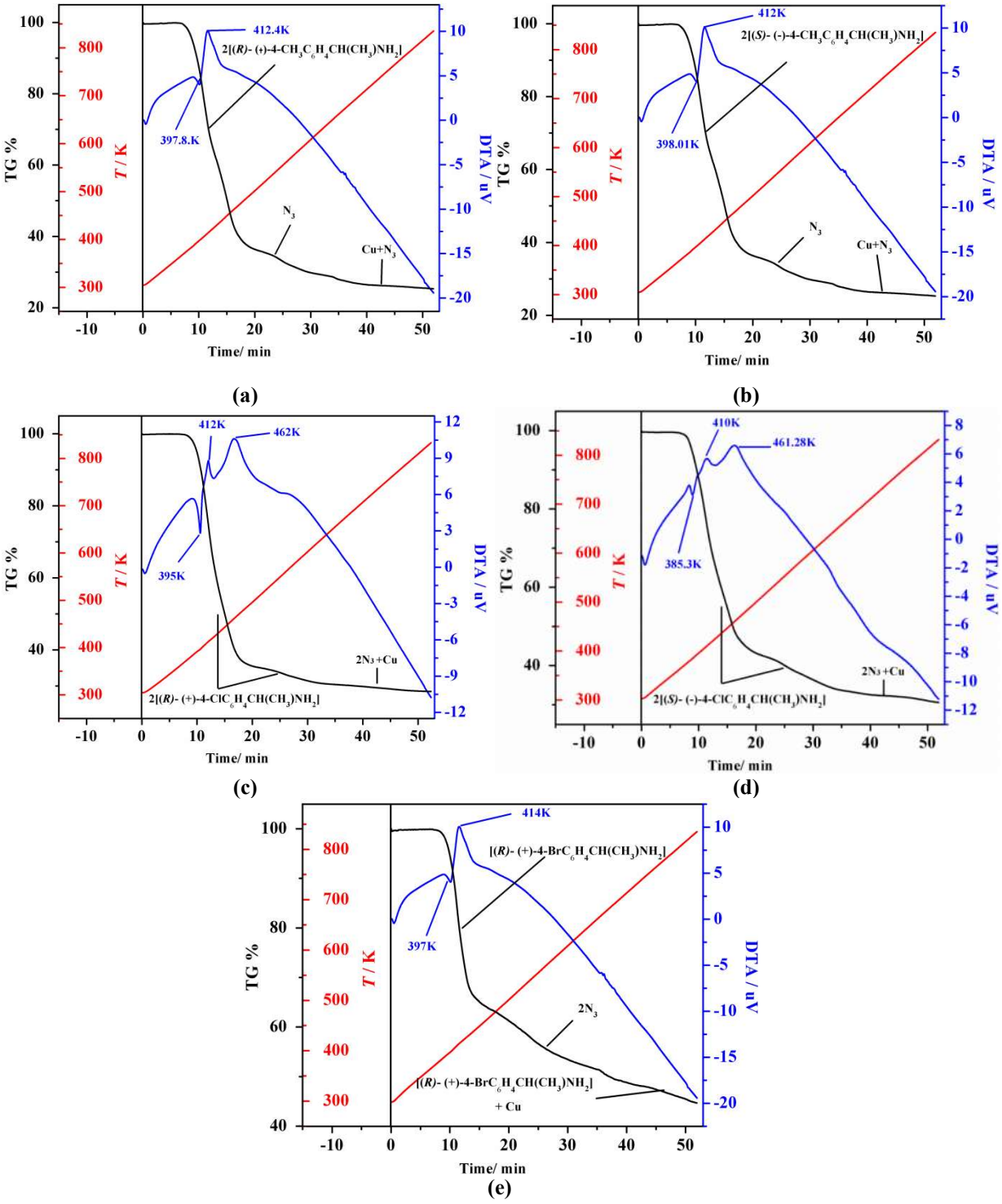

Fig. 2.2: TG-DTA of compound (a) 1, (b) 2, (c) 3, (d) 4 and (e) 5

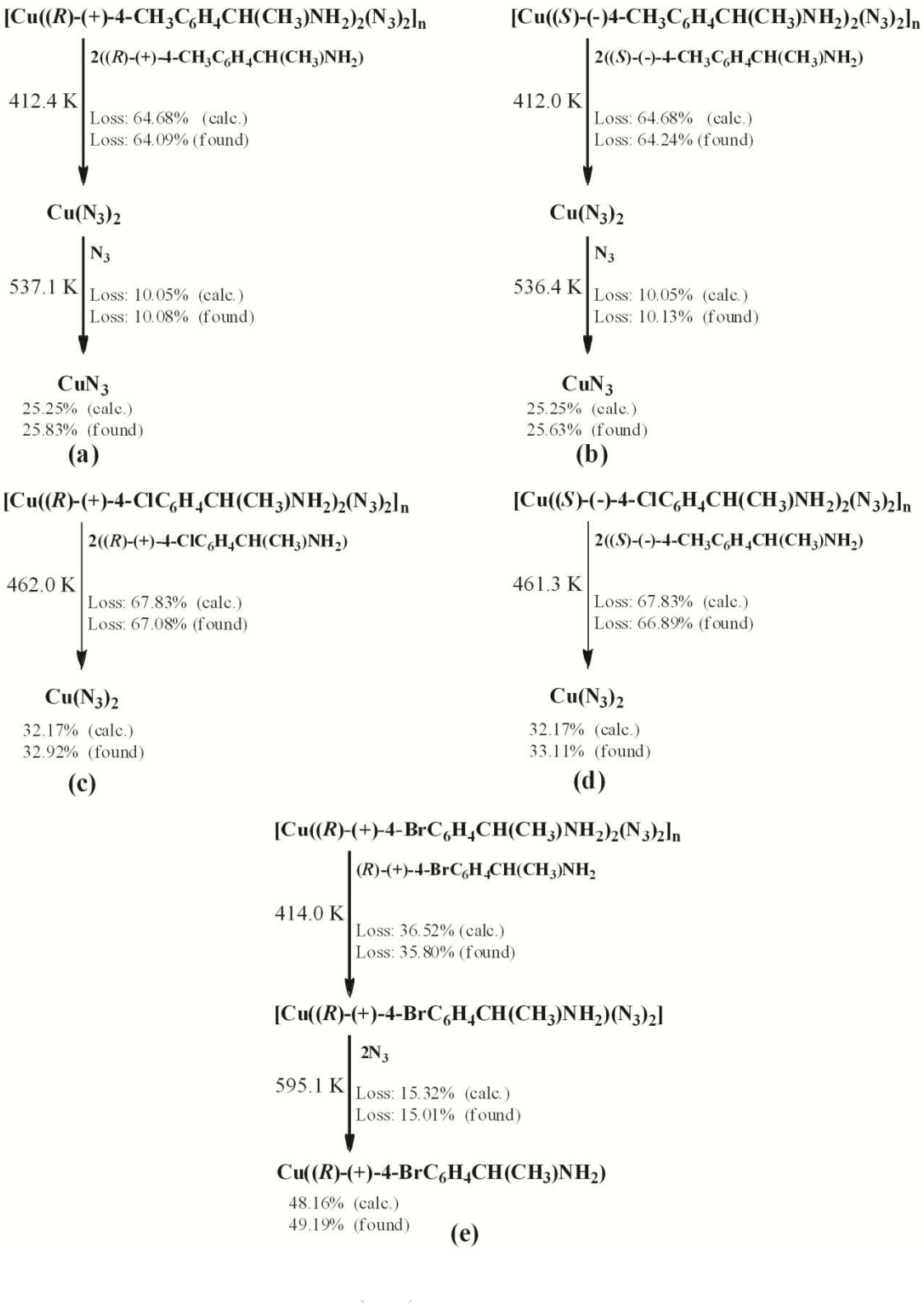

Fig. 2.3: Degradation pattern of compound (a) 1, (b) 2, (c) 3, (d) 4 and (e) 5

Compound **1-4** showed similar decomposition pattern while compound **5** shows different decomposition pattern, as shown in Figure 2.2 and 2.3. All compounds **1-5** are stable up to 370K. Compounds **1**, **2** and **3**, **4** shows the loss of both organic ligand in the range of 370-478K ((for **1**- Obsd. 64.09 %, Calcd. 64.68 %), ((for **2**- Obsd. 64.24 %, Calcd. 64.68 %)) and 370-637K ((for **3**- Obsd. 67.08 %, Calcd. 67.83 %), ((for **4**- Obsd. 66.89 %, Calcd. 67.83 %)) respectively. Then loss of two azide molecule took place. Compound **5** showed the slightly different degradation pattern. The loss of single organic ligand (Obsd. 35.80 %, Calcd. 36.52 %) in the range of 370- 489K, followed two molecules of azide (Obsd. 15.01 %, Calcd. 15.32 %) in the range of 490- 700K. The remaining product at high temp is probable Cu in all the compounds.

The DTA curves of **1, 2, 3, 4** and **5** indicate that the decomposition of the compound took place with one endothermic peak at 397.8K, 398K, 395K, 385.3K and 397K respectively. One exothermic peak observed in case of **1**, **2** and **3** at 412.4K, 412K and 414K respectively while two exothermic effects (crystallization, desolvation/dehydration) observed at 412K and 462K in case of **3** and 410K and 461.28K in case of **4**.

2.5 Spectral Information

2.5.1 UV-Visible Spectra:

UV- Visible spectrum recorded in solid state, in KBr pellet, showed distinct *d-d* transition at 450-500 nm. Apart from this, it showed three absorption bands, one strong absorption band at 230 while two bands at 300, and 466 nm for **1**, **2** and 295 and 451 nm for compounds **3**, **4** and **5** (Figure 2.4).

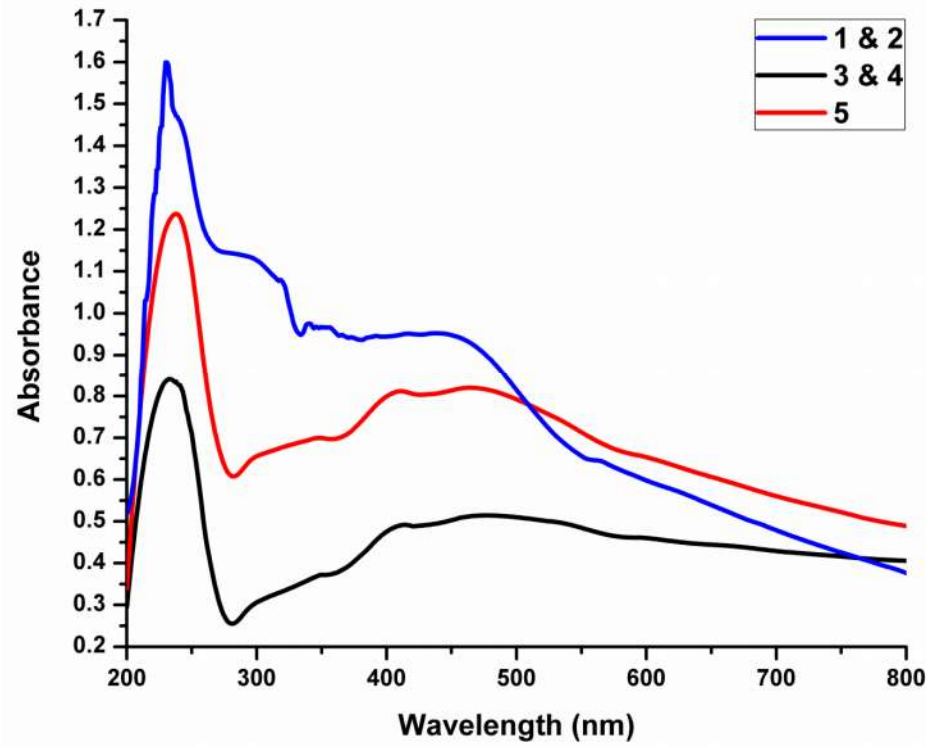

Fig. 2.4: Solid state absorption spectra of compound (a) 1, (b) 2, (c) 3, (d) 4 and (e) 5

2.5.2 CD Spectra:

Circular dichroism (CD) spectrum measurements of ligands in methanol and compounds in KBr pellets were carried out as shown in Figure 2.5.

All the compounds, **1-5,** display similar dichroic signals in CD spectra with respect to absorption frequencies observed in solid state UV-vis experiments (Figure 2.4). CD spectra of compounds show and confirm presence of *d-d* transition.

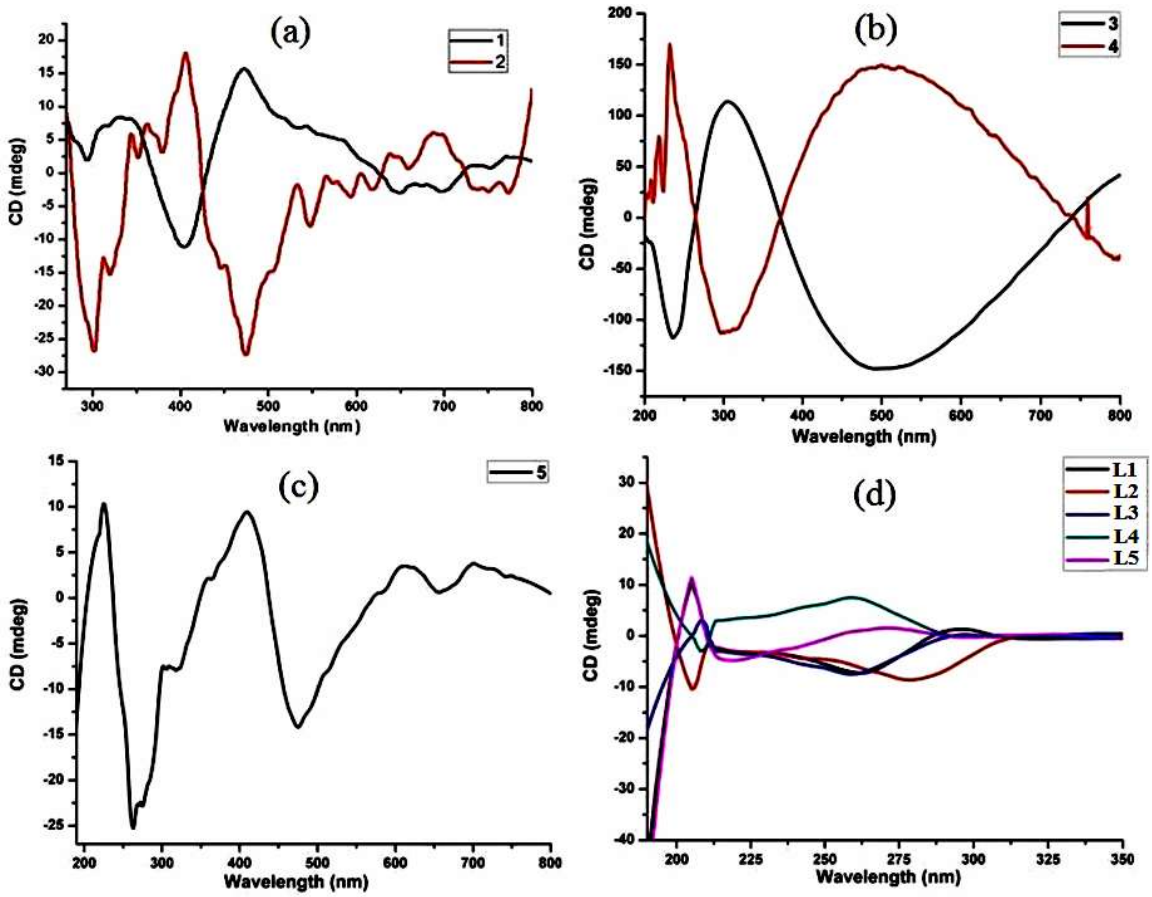

Fig. 2.5: (a) Solid CD spectra of 1 and 2 in KBr pellet, (b) Solid CD spectra of 3 and 4 in KBr pellet, (c) Solid CD spectra of 5 in KBr pellet and (d) CD spectra of Ligands (*R*)-(+)-4-methyl-*α*-methyl benzylamine (L1), (*S*)-(-)-4-methyl-*α*-methyl benzylamine (L2), (*R*)-(+)-4-chloro-*α*-methyl benzylamine (L3), (*S*)-(-)-4-chloro-*α*-methyl benzylamine (L4), (*R*)-(+)-4-bromo-*α*-methyl benzylamine (L5).

Compound **1** (*R*- isomer) showed positive Cotton effects at λ_{max} = 308 and 472 nm and negative cotton effect at 404 nm while **2** (*S*- isomer) exhibits a negative Cotton effect at λ_{max} = 305nm and 473 nm and a positive dichroic signal centred at 405 nm. While compound 3 (*R*- isomer) exhibits positive Cotton effects at λ_{max} = 232 and 503 nm and negative cotton effect at 299 nm, while compound **4** (*S*-isomer) shows Cotton effects with opposite signs at the same wavelength. The compound **5** (*R*- isomer) exhibits positive Cotton effects at λ_{max} = 224 and 409 nm and negative cotton effect at 264 nm.

Thus, results of circular dichroism (CD) spectrum measurements of ligands in methanol (Figure 2.2d) and compounds in KBr pellets further confirm the optical activity and enantiomeric nature of ligand and compounds.

2.6 Crystal structure

Single crystal XRD confirms the formation of compounds and crystals. The molecular structure of **1**, **2**, **3**, **4** and **5** are shown in Figure 2.6-2.8.

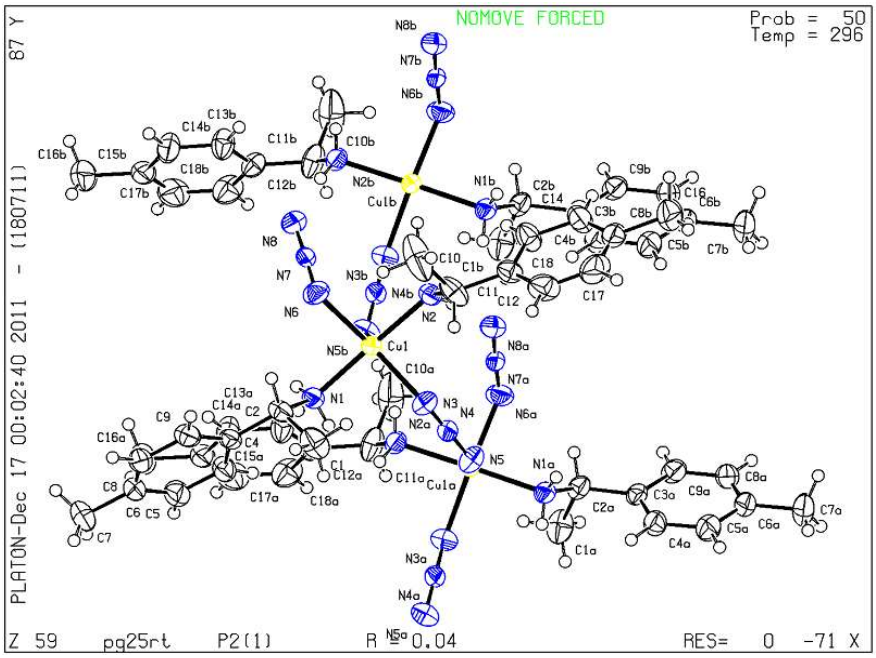

(a)

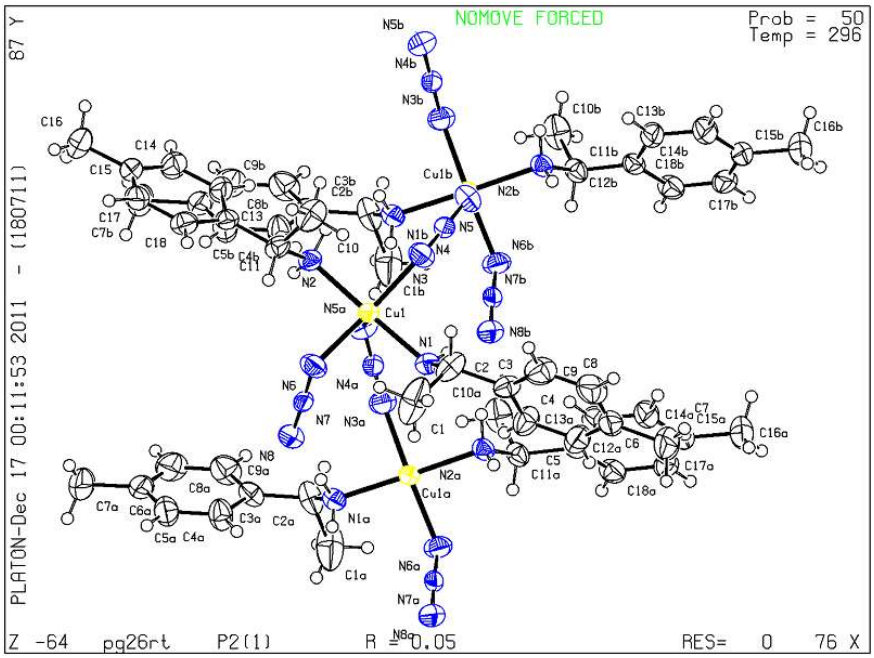

(b)

Fig.2.6: Molecular view of compound 1 (a) and compound 2 (b) having thermal ellipsoid are shown at 50 % probability

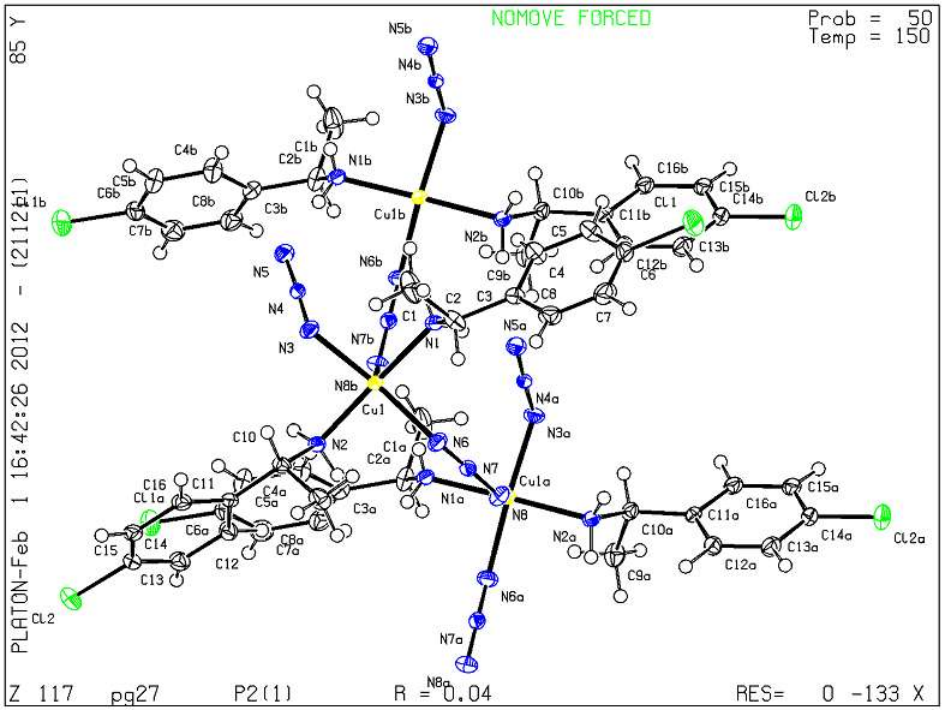

(a)

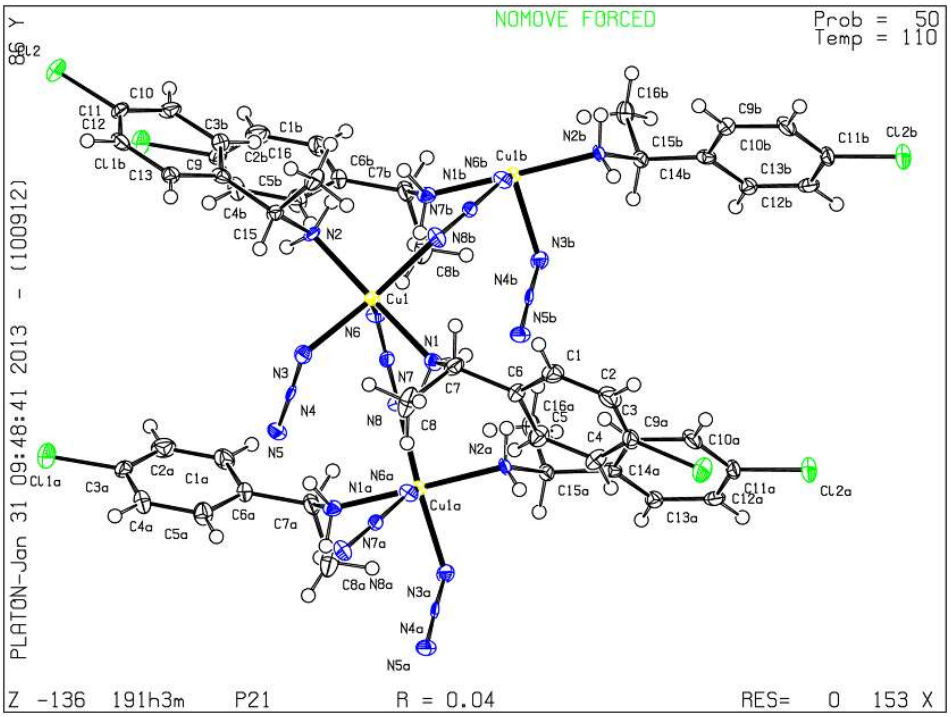

(b)

Fig.2.7: Molecular view of compound 3 (a) and compound 4 (b) having thermal ellipsoid are shown at 50 % probability

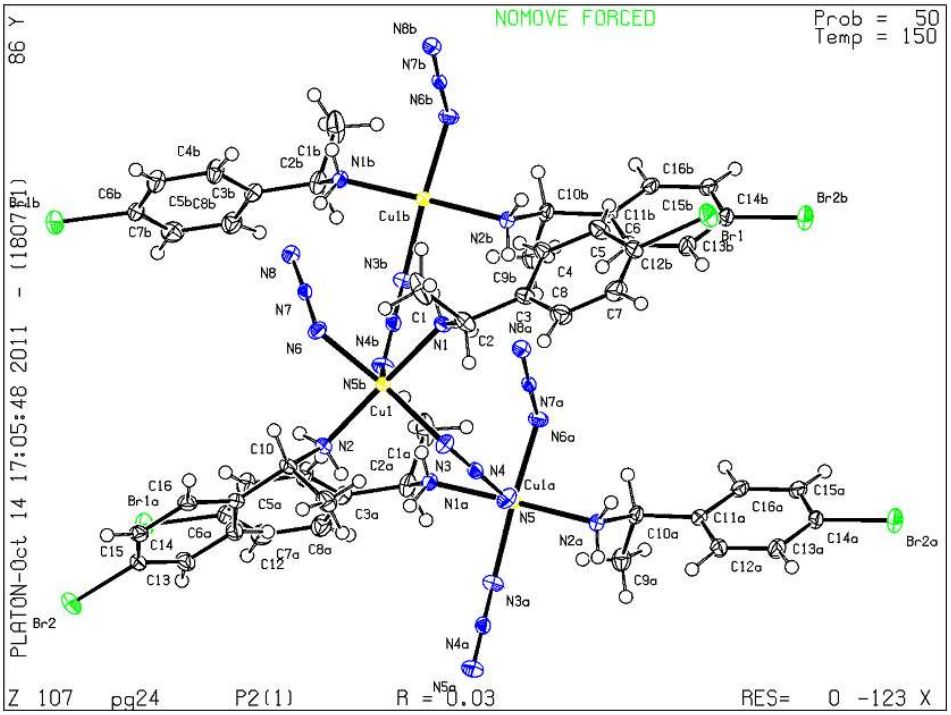

Fig.2.8: Molecular view of compound 5 having thermal ellipsoid are shown at 50 % probability

Table 2.1: Crystallographic data and structure refinements for compounds 1, 2, 3, 4 and 5

	1	2	3	4	5
Empirical formula	$C_{18}H_{26}CuN_8$	$C_{18}H_{26}CuN_8$	$C_{16}H_{20}Cl_2CuN_8$	$C_{16}H_{20}Cl_2CuN_8$	$C_{16}H_{20}Br_2CuN_8$
Formula weight	418.01	418.01	458.84	458.84	547.76
Wavelength	0.71073 Å	0.71073 Å	0.71073 A	0.71073 A	0.71073 Å
Crystal system	Monoclinic	Monoclinic	Monoclinic	Monoclinic	Monoclinic
Space group	$P2_1$	$P2_1$	$P2_1$	$P2_1$	$P2_1$
Unit cell dimensions	a = 11.7698(3)Å b = 7.4184(2) Å c = 12.7549(3)Å β = 110.052(1)°	a = 11.777(3) Å b = 7.4268(2) Å c = 12.771(3) Å β = 09.846(16)°	a = 11.7473(5)Å b = 7.3575(4) Å c = 12.7693(6)Å β =110.051(3)°	a = 11.591(4) Å b = 7.286(3) Å c = 12.709(5) Å β = 109.591(6)°	a = 11.5685(4)Å b = 7.3355(2) Å c = 12.9121(4)Å β = 100.80(2)°
Volume	1046.16(5) $Å^3$	1050.7(4) $Å^3$	1036.76(9) $Å^3$	1011.1(7) $Å^3$	1029.13(6) $Å^3$
Z	2	2	2	2	2
Density (calculated)	1.327 Mg/m^3	1.321 Mg/m^3	1.470 Mg/m^3	1.507 Mg/m^3	1.768 Mg/m^3
Absorption coefficient	1.063 mm^{-1}	1.058 mm^{-1}	1.329 mm^{-1}	1.363 mm^{-1}	4.962 mm^{-1}
Reflections collected	12052	12094	5735	5156	11261
Independent reflections	7286[R(int) = 0.0288]	7796 [R(int) = 0.0349]	4327 [R(int) = 0.0337]	3819 [R(int) = 0.0242]	6865 [R(int) = 0.0279]
Refinement method	Full-matrix least-squares on F2	Full-matrix least-squares on F2	Full-matrix least-squares on F2	Full-matrix least-squares on F2	Full-matrix least-squares on F2
Data / restraints / parameters	7286/1/260	7796 / 1 / 260	4327 / 1 / 311	3819 / 1 / 246	6865 / 1 / 324
Goodness-of-fit on F2	0.959	0.957	0.998	1.131	0.873
Final R indices [I>2sigma(I)]	R1 = 0.0378 wR2 = 0.0711	R1 = 0.0493 wR2 = 0.0802	R1 = 0.0404 wR2 = 0.0859	R1 = 0.0430 wR2 = 0.0924	R1 = 0.0317 wR2 = 0.0581
R indices (all data)	R1 = 0.0589 wR2 = 0.0781	R1 = 0.0945 wR2 = 0.0931	R1 = 0.0559 wR2 = 0.0937	R1 = 0.0453 wR2 = 0.0943	R1 = 0.0458 wR2 = 0.0627
Absolute structure parameter	0.013(10)	0.005(13)	0.026(15)	0.073(16)	0.019(6)

(*R/S*)-Methyl benzylamine crystallizes in chiral space group $P2_12_12_1$ (orthorhombic), is reported in the literature [13]. It forms neutral 2D brick-wall layers with a repeating azido-bridged eight membered copper brick. Here Cu (II) found to exist in three different environments, two with square pyramidal and one with square planar geometry, which are connected through only EO azido bridges. This is due to the fact that auxiliary ligand coordinates to only latter Cu centre that is square planar geometry. Surprisingly substituent at benzylic position, such as ethyl does not affect the 2D structure of the complex. It only gives rise to large interlayer distances of 13.200 and 13.738 Å in case of methyl and ethyl respectively. It is observed that an auxillary ligand remain self assembled in opposite direction between these layers without any π–π stacking and hydrogen-bond interactions. That means, substitution at benzyl position increases the interlayer distances only.

Interestingly substitution at phenyl ring (-Me), a present of compounds, changes the dimensionality of compounds from 2D to 1D. Various substituent's have incorporated to confirm the dimensionality change due to substituent effect which is thoroughly discussed here.

Crystallographic structural data for **1**, **2**, **3**, **4** and **5** reveal very similar features for the compounds, where compounds **1** and **2**, **3** and **4** are a pair of enantiomers. These compounds crystallize in the chiral space group $P2_1$, with absolute structure parameters of 0.013(10)-**1** and 0.005(13)-**2**, 0.026(15)-**3**, 0.073(16)-**4**, 0.014(17)-**5** respectively.

Surprisingly, these structures are quite different from that of the closely related $[Cu_3((R/S)\text{- mba})_2(N_3)_6]_n$, and forms 1-D helical network (Figure 2.6-2.8), proving change in the self assembly process. Among these compounds methyl and halides (-Cl, -Br) form interesting helical network with the *coexistence of both left-handed and right-handed helical chains*. Throughout the series, hydrogen bonds, CH···π interactions, and other intermolecular interactions play crucial role in stabilizing the resulting networks. Detail description of all these crystal described below.

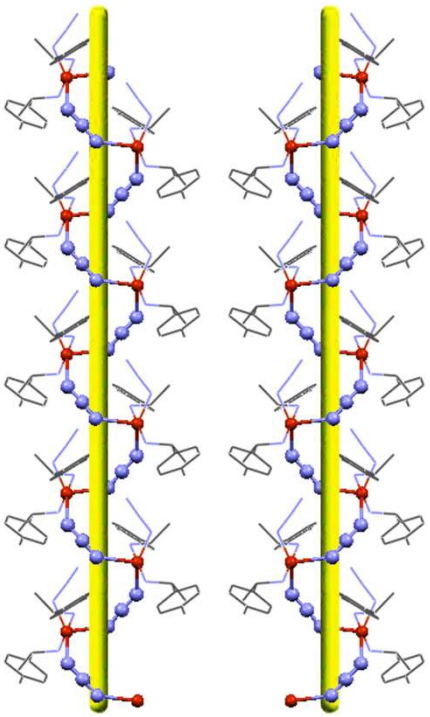

Fig. 2.9: Left handed and right handed helix motif

The crystal structure of all compounds shows a neutral helical chain in which the Cu^{II} ion is five nitrogen coordinated in the form of a distorted square based pyramid, CuN_5 (Figure 2.9).

The coordination sphere is composed of two CAL nitrogen atoms, a unidentate azide nitrogen atom and two *EE*-binding azide nitrogen atoms. CAL occupies two *trans* sites of the basal plane, and the other two *trans* sites are occupied by a bridging and unidentate azide ligands. The axial position is occupied by one nitrogen atom N(6) of the azide bridge in the *EE*- mode (Cu1-$N6_{axial}$; 2.333-2.377 Å) and the equatorial plane is formed by nitrogen atoms from the two amine ligands (Cu1-N1;1.997-2.011 Å , Cu1- N2;2.001-2.013 Å) and the nitrogen atom of the *EO* azide (Cu1- N3; 2.006- 2.009 Å). The N-N distances within a azide ion are not equal, axial azide (N6-N7) 1.171-1.185 Å and (N7-N8) 1.164-1.185 Å, and the difference between them is 0.009-0.015 Å. While the equatorial azide ((N3-N4) 1.186-1.193Å and (N4-N5) 1.157-1.167 Å), and the difference between them is 0.019-0.034 Å. The axial distance is larger than the corresponding equatorial one. The two coordinated ligand nitrogens make a trans angle of 178.38-

178.91° with central Cu ion. Similarly, the *EE* azide nitrogen (N8b) and *EO* azide nitrogen (N3) make an angle of 159.50-160.07°. Thus the geometry around copper ion can be best described as a highly distorted square pyramid.

The copper atom laid 0.185 Å above from the mean plane N1-N3-N2-N8. Each Cu^{II} centre is linked to another Cu^{II} centre by *EE* azide bridges to two neighbours leading to neutral network. The Cu1···Cu1a separation through *EE* azide bridge is 5.305-5.353 Å. For *EE* bridges, Cu1-N6-N7 angle is 128.43-135.05º and the Cu1-N8b-N7b is 127.86-133.94º; the EE azide is quasi linear (N6-N7-N8, 176.07-176.46º). For EO, Cu1-N3-N4 angle is 120.95-122.16º; the EO azide is also quasi linear (N3-N4-N5, 177.58-177.76º).

The helices are generated around the crystallographic 2_1 screw axes with neighbouring Cu···Cu distance of 5.305-5.353Å. In a pitch of helical chain the Cu1a···Cu1b distance is 7.286-7.427 Å. The distance between two pitch of adjacent helical chain in *ab* plane is 11.569-11.777 Å and in 12.709-12.912 Å in *bc* plane.

Structure of **1, 2** and **3, 4** are similar to each other, except for that the ligand L1 adopts a (*R*) configuration in **1** (Figure 2.6-a, b), and the connections of corresponding *via* the same intra- helical chain hydrogen bonds to generate a 1D left-handed helical chain, with N5b···N2*a,* N5b···C9a, N5b···N1b and N6···N2b hydrogen bonding distances of 3.081 Å, 3.454 Å, 3.037 Å and 3.162 Å respectively. While (*S*)-isomer (**2**) possess the opposite i.e. right handed helical chain demonstrating correlation between chirality and helicity of helical chains. The 1-D helices of compounds are further stabilized via inter-chain supramolecular interactions. In case of **1** and **2**, the helix is further stabilized via CH···π interactions [14] between two adjacent helices while in **3, 4** and **5** inter-chain weak X···N interaction between the halogen and terminal nitrogen atom of the EO azide with distance of (3.239 Å) (Figure 2.10 and Figure 2.11).

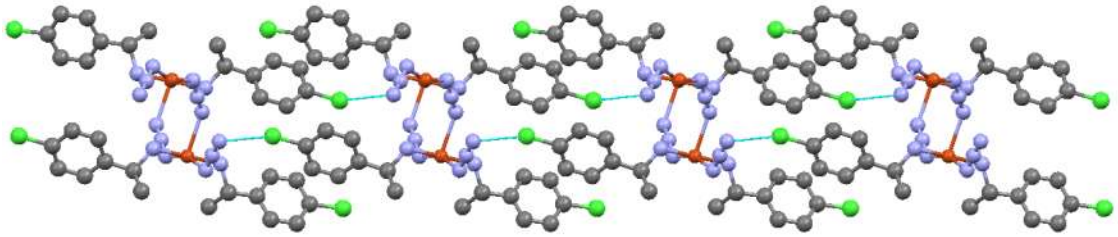

Fig. 2.10: Supramolecular Cl···N interactions present along the chains to stabilize Inter helical chain-3.239 Å

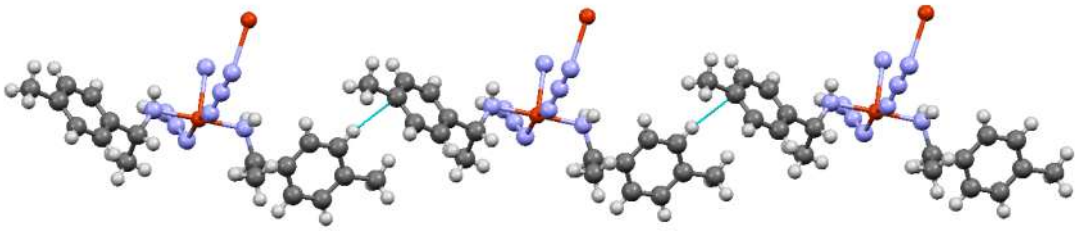

Fig. 2.11: Supramolecular C-H¨π interactions in 3 present along the adjacent chains to stabilize Inter helical chain

Each helical chain connects four adjacent helices through such supramolecular interactions, which make the neighbouring helices possess the same chirality (Figure2.12) Thus, complex **1-5** possesses a chiral supramolecular architecture due to the existence of supramolecular interactions between helical chains, through which the same chirality is preserved and transfer to whole crystal system. CD spectra also confirm the chirality. This result supports that there is a correlation between the chirality of the building blocks and the helicity of the 1-D helical chains constructed by these building blocks [15].

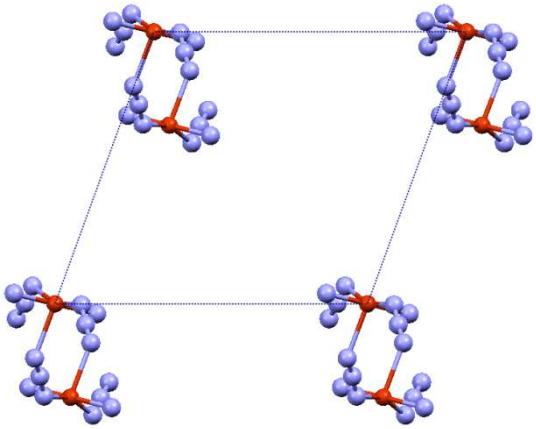

Fig. 2.12: Inter helical chain distances

We also observed two more weak interactions in the form of helical chains between, (a) *EO*-azide with CAL amine hydrogen (N5b···N1H and N5···N1aH, 3.037Å) to form an opposite helical chain with respect to main helical chain (Figure 2.13A); (b) *EE*-azide nitrogen and CAL amine hydrogen (N7bH···N6, 2.294 Å) via copper which is collinear with 2_1 screw axis (Figure 2.13B). Due to these extra helical chains the structure get further stabilised into one dimensional compare to reported benzylamine compounds.

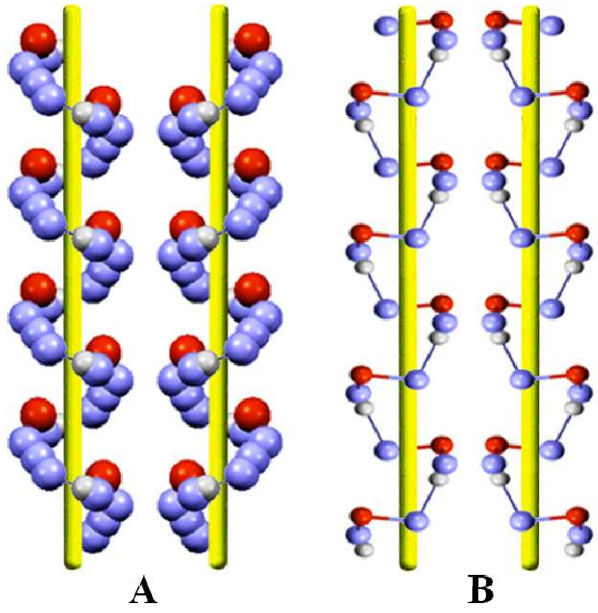

Fig. 2.13: Helical chains from supramolecular interactions

Thus, when enantiopure CAL **L1**, **L2**, **L3**, **L4** and **L5** were used self-assembly process forces bridging ligand to be only in *EE*-mode to communicate between adjacent metal centers for the formation of 1-D helical chain network leading to truly transforming chirality in the molecule to the bulk structure.

2.6 Mixed Ligand Approach

To check the effect of CAL-CAL interaction of ligand and overall on dimensionality of complex we synthesized compounds using admixture of (*R*)-(+)-4-Cl mba and (*R*)-(-)-mba (1:1) ligands.

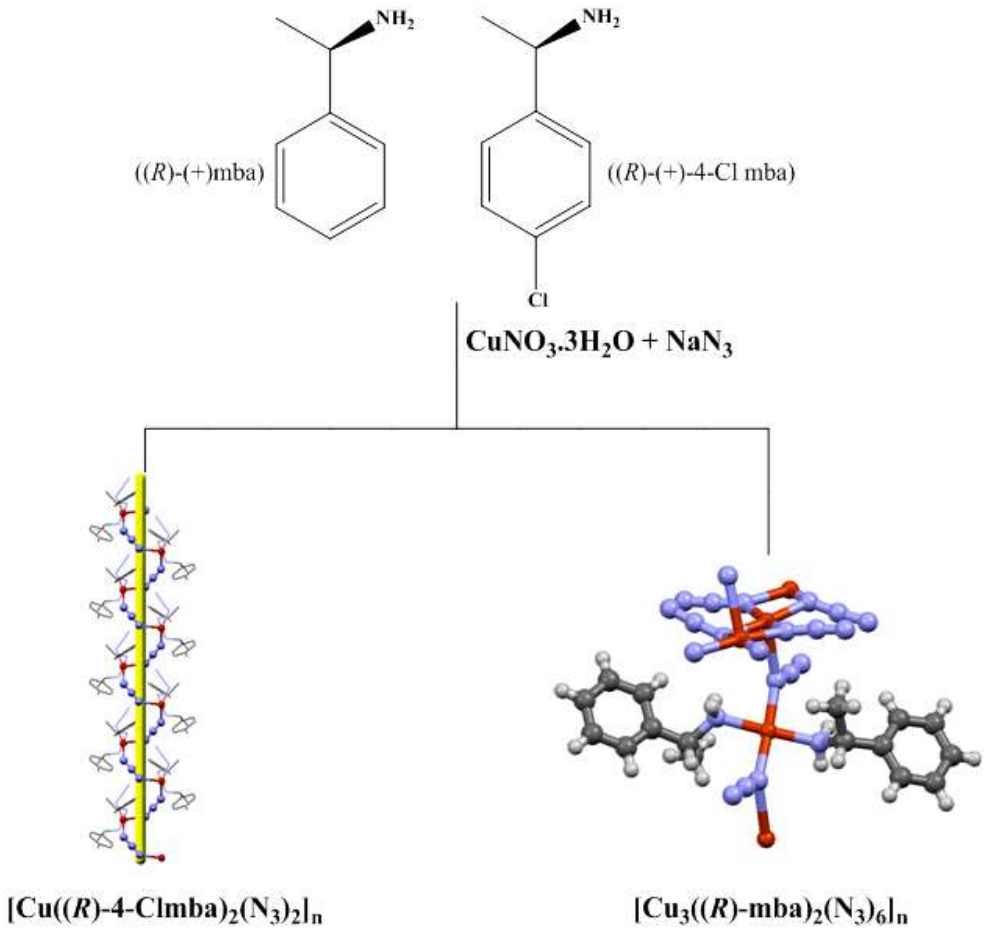

Interestingly we observed two types of crystals in this pot reaction. Crystals with 1D helical assembly with (*R*)-(+)-4-Cl mba ligand and 2D brick-wall layers assembly with (*R*)-(+)-mba suggest were present in equal ration. Self assembly driven crystal formation is confirmed since none of the crystal was found containing mixed ligands. Thus, CAL and hence spontaneity self-assembly process played an important role in the crystallization of these compounds. The ligand driven dimensionality of compounds confirms the importance of CAL-CAL interactions. Substitution away from chiral centre in ligands can enhance CAL-CAL interactions.

This one pot reaction was carried out at high temperature (50 °C) and low temperature (~0 °C) to crystallize thermodynamically or kinetically stable products, but *in vein*. That means the self-assembly process, although driven by CAL and bridging ligand, maintains the expression of individuality of the ligand during the overall crystallization process. The helicity depends upon enantiomeric isomer of ligand. The chirality of formed compounds has been confirmed by CD spectra.

2.7 Magnetic Study

Due to presence of end-to-end azide bridging, all compounds were expected to give antiferromagnetic coupling. The variable temperature magnetic measurements, using SQUID magnetometer, on Compounds **1 (2)** and **3 (4), 5** are presented in Figure 2.14-a,b,c. At 300K, $\chi_m T$ value for compound **1** is 0.1048 emu.K.mol^{-1}, for compound **3** is 0.08751 emu.K.mol^{-1} and 0.0889 emu.K.mol^{-1} for compound **5**. The value of $\chi_m T$ for all compounds is almost equal to value expected for Copper (II) ion (μ_{eff} = 0.83 BM, s = ½ and g = 2.00). When cooled up to 5K, χ_m value increases linearly for compound **1**, while showed rounded maxima around 20K and 16K was observed for compound **3** and **5**. The χ^{-1} *vs. T* plots obeys the Curie–Weiss law with a negative Weiss constant of θ = -161 K; for **1**, θ = -136.48K for **3** and θ = -134.10K for **5**. C_m values for **1**, **3** and **5** are 4.44, 4.08 and 5.00 emu.K.mol^{-1} respectively. The high negative value of θ and decreasing values of χmT suggest strong antiferromagnetic interactions between neighbouring Cu (II) ions through the N_3 bridges.

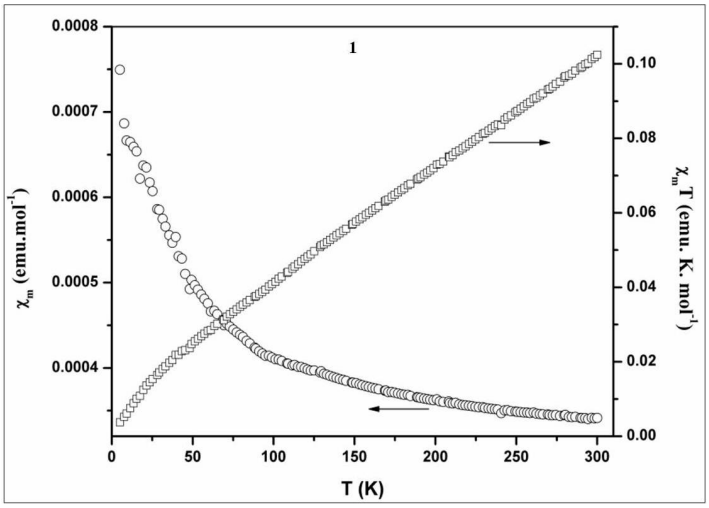

(a)

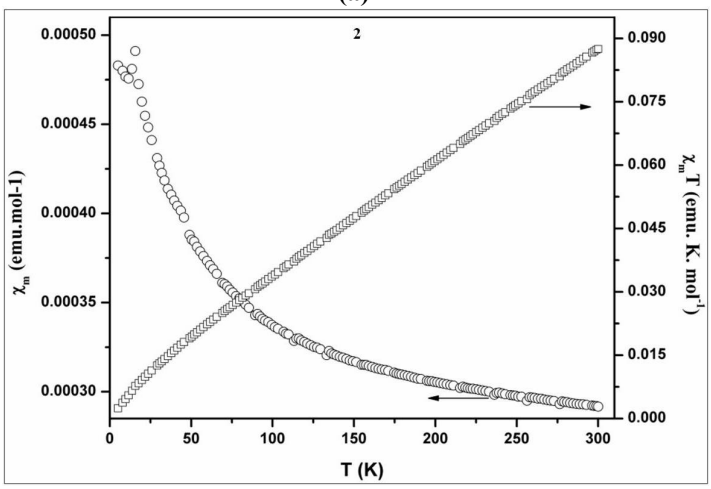

(b)

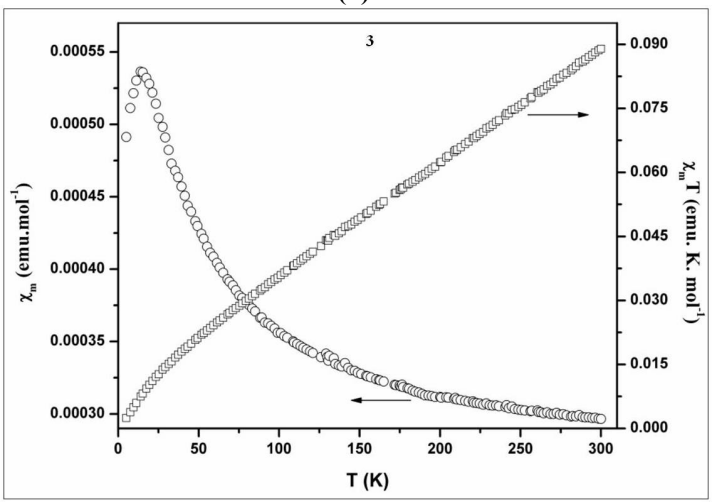

(c)

Fig. 2.14: Plots of χ_M *versus* T and $\chi_M T$ *versus* T for 1 (a), 3 (b) and 5 (c)

2.8 Conclusion

- Five new 1D helical compounds were synthesized and thoroughly characterised.
- Single crystal X-ray studies showed helicity in these compounds is driven by enantiomeric chiral building blocks.
- By a proper substitution in a molecule, away from chiral centre, one can enhance or trigger chiral ligand-chiral ligand interaction (CAL) in a self-assembly driven one pot crystal formation reaction to design multifunctional molecular magnets.
- CD spectroscopy confirms helicity in chiral ligand is expressed in final compound.
- SQUID magnetometric studies reveal that all these compounds showed antiferromagtic interaction due to *end-to-end* azide bridging between metal ions.
- The CAL- CAL interactions will not only play important role in crystal growth or dimensionality, but might help in tuning other physical behaviour. Detailed investigation in this direction is required.

2.9 References

[1] R. L. Carlin, *Magnetochemistry*, Springer Berlin *et al*., **1986**.

[2] S. Miller Joel, J. Epstein Arthur, in *Molecule-Based Magnetic Materials, Vol. 644*, American Chemical Society, **1996**, 1-13.

[3] J. S. Miller, M. Drillon, *Magnetism: Molecules to Materials IV*, John Wiley & Sons, **2006**.

[4] (a) J. S. Miller, J. C. Calabrese, H. Rommelmann, S. R. Chittipeddi, J. H. Zhang, W. M. Reiff, A. J. Epstein, *J. Am. Chem. Soc.* **1987**, *109*, 769-781; (b) O. Kahn, Y. Pei, M. Verdaguer, J. P. Renard, J. Sletten, *J. Am. Chem. Soc.* **1988**, *110*, 782-789.

[5] (a) S. L. James, *Chem. Soc. Rev.* **2003**, *32*, 276-288; (b) S. Kitagawa, R. Kitaura, S.-i. Noro, *Angew. Chem. Int. Ed.* **2004**, *43*, 2334-2375; (c) S. Lee, A. B. Mallik, Z. Xu, E. B. Lobkovsky, L. Tran, *Acc. Chem. Res.* **2005**, *38*, 251-261; (d) K. S. Suslick, P. Bhyrappa, J. H. Chou, M. E. Kosal, S. Nakagaki, D. W. Smithenry, S. R. Wilson, *Acc. Chem. Res.* **2005**, *38*, 283-291; (e) P. Feng, X. Bu, N. Zheng, *Acc. Chem. Res.* **2004**, *38*, 293-303; (f) J. L. C. Rowsell, O. M. Yaghi, B. Chen, N. W. Ockwig, A. R. Millward, D. S. Contreras, *Angew. Chem. Int. Ed.* **2005**, *44*, 4647-4647; (g) G G. Ferey, *Chem. Soc. Rev.* **2008**, *37*, 191-214; (h) M. P. Suh, Y. E. Cheon, E. Y. Lee, *Coord. Chem. Rev.* **2008**, *252*, 1007-1026; (i) Q. Yu, Y.-F. Zeng, J.-P. Zhao, Q. Yang, B.-W. Hu, Z. Chang, X.-H. Bu, *Inorg. Chem.* **2010**, *49*, 4301-4306; (j) S. Sasmal, S. Sarkar, N. r. Aliaga-Alcalde, S. Mohanta, *Inorg. Chem.* **2011**, *50*, 5687-5695.

[6] C. Train, M. Gruselle, M. Verdaguer, *Chem. Soc. Rev.* **2011**, *40*, 3297-3312.

[7] (a) J. Crassous, *Chem. Soc. Rev.* **2009**, *38*, 830-845; (b) J. Crassous, *Chem. Commun.* **2012**, *48*, 9687-9695 (c) T. Kawamoto, N. Suzuki, T. Ono, D. Gong, T. Konno, *Chem. Commun.* **2013**, *49*, 668-670; (d) Z.-Z. Li, S.-Y. Yao, J.-J. Wu, B.-H. Ye, *Chem. Commun.* **2014**, *50*, 5644-5647.

[8] (a) S. Chorazy, K. Nakabayashi, K. Imoto, J. Mlynarski, B. Sieklucka, S.-i. Ohkoshi, *J. Am. Chem. Soc.* **2012**, *134*, 16151-16154; (b) E. Pardo, C. Train, R. Lescouezec, Y. Journaux, J. Pasan, C. Ruiz-Perez, F. S. Delgado, R. Ruiz-Garcia, F.

Lloret, C. Paulsen, *Chem. Commun.* **2010**, *46*, 2322-2324; (c) J. Ferrando-Soria, D. Cangussu, M. Eslava, Y. Journaux, R. Lescouëzec, M. Julve, F. Lloret, J. Pasán, C. Ruiz-Pérez, E. Lhotel, C. Paulsen, E. Pardo, *Chem. Eur. J.* **2011**, *17*, 12482-12494.

[9] (a) M. Eddaoudi, D. B. Moler, H. Li, B. Chen, T. M. Reineke, M. O'Keeffe, O. M. Yaghi, *Acc. Chem. Res.* **2001**, *34*, 319-330; (b) M. Eddaoudi, J. Kim, N. Rosi, D. Vodak, J. Wachter, M. O'Keeffe, O. M. Yaghi, *Science* **2002**, *295*, 469-471; (c) N. W. Ockwig, O. Delgado-Friedrichs, M. O'Keeffe, O. M. Yaghi, *Acc. Chem. Res.* **2005**, *38*, 176-182.

[10] (a) J. Ribas, M. Monfort, X. Solans, M. Drillon, *Inorg. Chem* **1994**, 33, 742-745; (b) T. K. Maji, P. S. Mukherjee, G. Mostafa, T. Mallah, J. Cano-Boquera, N. R. Chaudhuri, *Chem. Commun* **2001**, 1012-1013 (c) K. Inoue, H. Imai, P. S. Ghalsasi, K. Kikuchi, M. Ohba, H. Ōkawa, J. Yakhmi, *Angew. Chem. Int. Ed.*, **2001**, *40*, 4242-4245 (d) H.-R. Wen, Y.-Z. Tang, C.-M. Liu, J.-L. Chen, C.-L. Yu, *Inorg. Chem.* **2009**, *48*, 10177-10185; (e) Magnetism: Molecules to Materials V Ed. J. S. Miller, M. Drillon, (**2005**) Wiley-VCH Verlag GmbH & Co. KGaA Weinheim, Germany. (f) X.-D. Zheng, Y.-L. Hua, R.-G. Xiong, J.-Z. Ge, T.-B. Lu, *Cryst. Growth Des.* **2011**, *11*, 302-310; (g) S. Mukherjee, P. S. Mukherjee, *Acc. Chem. Res.* **2013**, *46*, 2556-2566.

[11] Most of the azide mediated molecular magnet procedures use NaN_3 in quite large excess, minimum 10 times, in order to have high nuclearity or nucleation in the final complex.

[12] Z. Shen, J.-L. Zuo, S. Gao, Y. Song, C.-M. Che, H.-K. Fun, X.-Z. You, *Angew. Chem.* **2000**, *39*, 3633-3635.

[13] (a) Z.-G. Gu, Y. Song, J.-L. Zuo, X.-Z. You, *Inorg. Chem.* **2007**, *46*, 9522- 9524.; (b) Z.-G. Gu, Y.-F. Xu, X.-J. Yin, X.-H. Zhou, J.-L. Zuo, X.-Z. You, *Dalton Trans.* **2008**, 5593-5602.

[14] K. M. Sureshan, T. Uchimaru, Y. Yao, Y. Watanabe, *Cryst. Eng. Comm.* **2008**, *10*, 493-496.

[15] (a) H.-Y. An, E.-B. Wang, D.-R. Xiao, Y.-G. Li, Z.-M. Su, L. Xu, *Angew. Chem. Int. Ed.* **2006**, *45*, 904-908; (b) G.-C. Ou, L. Jiang, X.-L. Feng, T.-B. Lu, *Inorg. Chem.* **2008**, *47*, 2710-2718; (c) X.-D. Zheng, L. Jiang, X.-L. Feng, T.-B. Lu, *Dalton Trans.* **2009**, 6802-6808; (d) H.-Y. Li, L. Jiang, H. Xiang, T. A. Makal, H.-C. Zhou, T.-B. Lu, *Inorg. Chem.* **2011**, *50*, 3177-3179.